J. Rubb. Res., **7(2)**, 79–103

Non-linear Rate-dependent Hysteresis Model for Structural Dampers Made from Ultra-high Damping Natural Rubber

K.-S. LEE*#, R. SAUSE*, J. RICLES*, KAMARUDIN AB-MALEK** AND L.-W. LU*

It is well known that rubber-like materials exhibit non-linear behaviour that depends on strain amplitude, ambient temperature, and loading frequency. Comprehensive experimental tests were performed to investigate the non-linear behaviour of a newly developed damping material for structural dampers, ultra-high damping Natural Rubber (UHDNR). The structural dampers currently used to reduce the dynamic response of buildings and similar structures are rarely made from rubber-like materials, but are sometimes made from viscoelastic materials. Compared to a typical viscoelastic material, it has been observed that the UHDNR material is less dependent on loading frequency and ambient temperature but has sufficient damping for application in structural dampers A rate-dependent hysteresis model considering the strain amplitude and loading frequency dependence is proposed. Good agreement was observed between experimental and analytical results

Key words: behaviour; strain; amplitude; loading; frequency; experimental; tests; ultra-high; Natural Rubber; ambient temperature; structural; dampers; rate-dependent; hysteresis; model

Ultra-high Damping Natural Rubber (UHDNR) material is a rubber material developed for application in structural dampers that are used to damp dynamic response of buildings and similar structures. UHDNR has several advantages as an energy dissipation material for structural dampers. First, the mechanical properties of UHDNR, stiffness and energy dissipation, are less dependent on loading frequency and ambient temperature than the viscoelastic materials that are used in structural dampers. Second, the temperature increase in UHDNR material during dynamic loading is relatively small. As a result, the changes in the mechanical properties due to this temperature increase are negligible. Finally, UHDNR recovers its original mechanical properties after a short relaxation time if excessive strains are not applied. Based on these characteristics, UHDNR has the potential to be an excellent material for structural dampers.

Experimental tests were performed on UHDNR dampers and a loading rate-independent model has been developed by Sause and

*Department of Civil and Environmental Engr., ATLSS Center, Lehigh University, Bethlehem, PA 18015, USA
**Rubber Research Institute of Malaysia, Malaysian Rubber Board. P.O. Box 10150, 50908 Kuala Lumpur, Malaysia
#Corresponding author: (E-mail: ksl2@lehigh.edu)

co-researchers. (2001). Similar to other hysteresis models for the non-linear behaviour of High Damping Natural Rubber (HDNR), such as those of Ahmadi *et al.*[2] and Kikuchi and Aiken[3], the rate-independent model developed by Sause *et al.*[1] is based on the strain dependent behaviour observed in experimental tests at 0.5 Hz loading frequency and 20°C ambient temperature. As a result, the effects of variations in ambient temperature and loading frequency are not considered in the loading rate-independent model.

Numerous experimental tests were performed to investigate the dependence of UHDNR on ambient temperature and loading frequency in addition to strain amplitude[4]. This paper summarises data from experiments on small-scale prototype UHDNR dampers under various ambient temperatures and loading frequencies, and presents a loading rate-dependent model which can accurately predict the behaviour of UHDNR dampers.

EXPERIMENTAL TESTS

A small-scale structural damper that consist of two layers of UHDNR material bonded between three steel plates is depicted in *Figure 1a* . When the forces are applied in the axial direction of the plates, the layers of UHDNR deform in shear, resulting in energy dissipation in a form of heat. The dampers were fabricated at the Malaysian Rubber Board and were tested at the ATLSS Center at Lehigh University. The thickness of the UHDNR material in the small-scale structural damper is 10 mm, and the width and length are 100 mm making the shear area equal to 10 000 mm^2. The width and length of each steel plate is 100 mm and 200 mm. *Figure 1b* shows a UHDNR damper installed in the Material Test System 810 that was used to apply displacement histories to the UHDNR dampers. Two external displacement transducers were used to verify the displacement histories.

The experimental tests were focused on the dependence of UHDNR stress-strain behaviour on strain amplitude, ambient temperature, and loading frequency. The UHDNR dampers were subjected to sinusoidal displacement histories with ten complete cycles. Each displacement history produced a specified shear strain amplitude. The strain amplitude ranged from 20% to 100% strain with a 10% strain increment between each history. At the end of each history at a specified strain amplitude, the UHDNR damper was left at rest for one minute, and, thereafter, the displacement history for the next strain amplitude was applied. The tests were performed at 5 different ambient temperatures, 0°C, 10°C, 20°C, 30°C, and 40°C to investigate the ambient temperature dependence. A temperature chamber shown in *Figure 1c* was used to maintain the target temperature during the test. Two thermocouples were embedded in the UHDNR material to a 25 mm depth to monitor the temperature inside of the UHDNR material. *Figure 1d* shows the thermocouples embedded in the UHDNR material. For the 0°C and 10°C temperatures, cold air generated from dry ice was blown into the temperature chamber using an air fan, and the temperature change in the UHDNR material was monitored by the thermocouples. After detecting that the UHDNR material was stable at the target temperature, the set of displacement histories (producing 20% to 100% strain amplitude with a 10% strain increment) was applied. For the 30°C and 40°C temperatures, hot air was blown into the temperature chamber and the same procedures were followed. The sinusoidal displacement histories were applied at a 0.5 Hz loading frequency for each ambient temperature.

COPYRIGHT © MALAYSIAN RUBBER BOARD

(a) Configuration of structural damper.

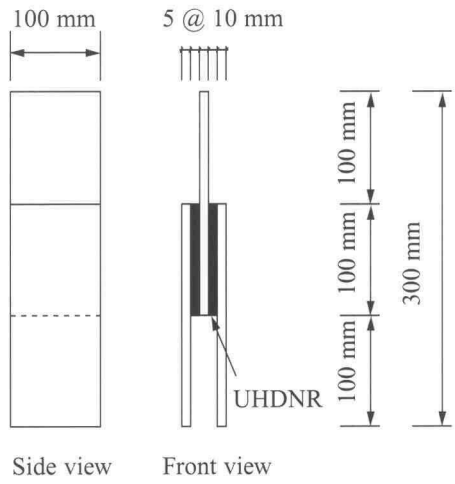

(b) Experimental test Set-up.

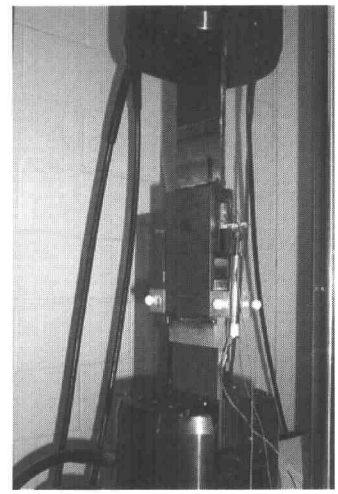

(c) UHDNR damper enclosed in temperature chamber.

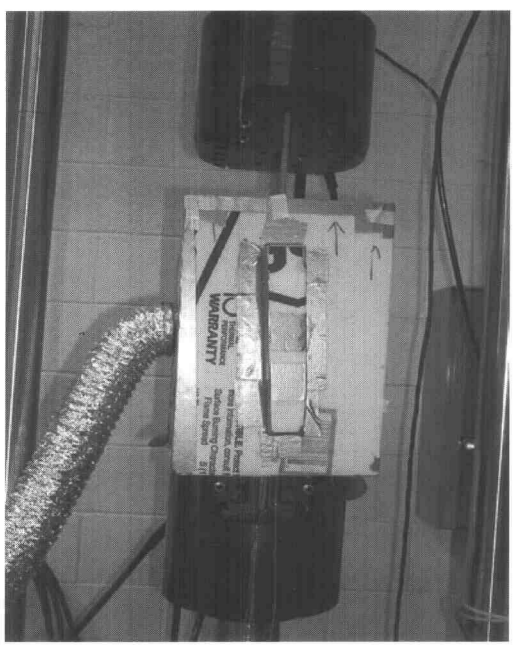

(d) Thermocouples embedded in UHDNR.

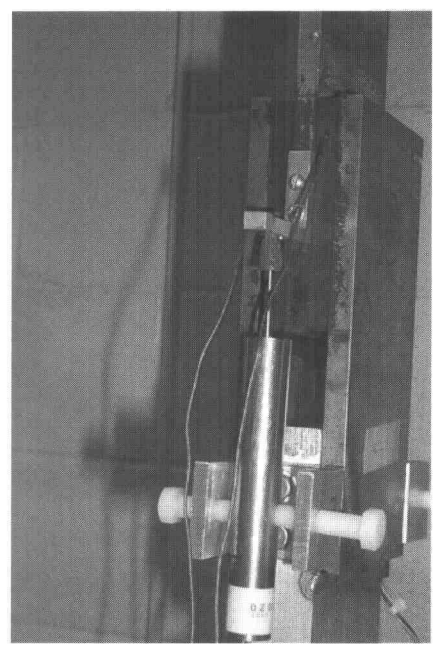

Figure 1. Configuration of structural damper made from UHDNR and experimental test set-up.

In order to investigate the influence of loading frequency, four loading frequencies, 0 5 Hz, 0 75 Hz, 1 Hz, and 1 5 Hz, corresponding to fundamental frequencies of low to medium rise buildings, were considered in this study Sinusoidal displacement histories of 10 complete cycles corresponding to 25%, 50%, 75%, and 100% shear strain amplitudes were applied at each loading frequency The ambient temperature for the frequency dependence tests was maintained near 20°C

Mechanical properties of UHDNR

The shear modulus and loss factor are often used to define the mechanical properties (stiffness and energy dissipation capacity) of damping materials The shear stress-strain hysteresis loops of the UHDNR material are not ellipses like those of viscoelastic materials, so an idealisation which replaces the non-linear hysteresis loops of UHDNR with ellipses is used Generally, two criteria are used to idealise damping materials in this manner[5] (1) similarity of the maximum stress and strain values, and (2) similarity of the hysteresis loop area The equivalent shear modulus, G_{eq}, which represents the material stiffness, is defined as the ratio of the maximum stress to the maximum strain The equivalent loss factor $\tan(\delta)$, which represents the material energy dissipation capacity is determined by the following equation

$$\tan(\delta) = \frac{ED}{2\pi ES} \qquad 1$$

where ED = the energy dissipated per cycle of sinusoidal loading and
ES = the maximum strain energy stored in a cycle of sinusoidal loading

ED can be determined by integration of the hysteresis loops and ES can be calculated from the maximum stress and strain A detailed discussion can be found in Sause *et al* [1] on the equivalent shear modulus and loss factor for the UHDNR material

Effects of Ambient Temperature and Strain Amplitude

The hysteresis loops for the UHDNR dampers tested at five different ambient temperatures at a loading frequency of 0 5 Hz are shown in *Figure 2* As shown, the hysteresis loops are stiffer and fatter as the ambient temperature decreases The hysteresis loops in *Figure 2a* from a test at 0°C have the largest stiffness and the greatest energy dissipation The hysteresis loops in *Figure 2e* from a test at 40°C have the smallest stiffness and the least energy dissipation

The mechanical properties of UHDNR are summarised in *Figure 3* for various temperatures and strain amplitudes As shown in *Figure 3a*, increasing the ambient temperature makes the UHDNR damper more flexible A significant decrease in the equivalent shear modulus (stiffness) is observed when the ambient temperature increases from 0°C to 10°C, but there is no distinct difference in stiffness between 30°C and 40°C The equivalent shear modulus at 20% strain amplitude and 0°C is 1 319 MPa, which is about 2 04 times greater than at 20% strain amplitude and 40°C (0 646 MPa) For other strain amplitudes, the equivalent shear modulus at 0°C is 1 92 to 1 65 times greater than at 40°C The temperature dependence is more significant for small strain amplitudes (*e g* 20%), and decreases as the strain amplitude increases The equivalent loss factor, shown in *Figure 3b*, decreases as the ambient temperature increases, but is less dependent on ambient

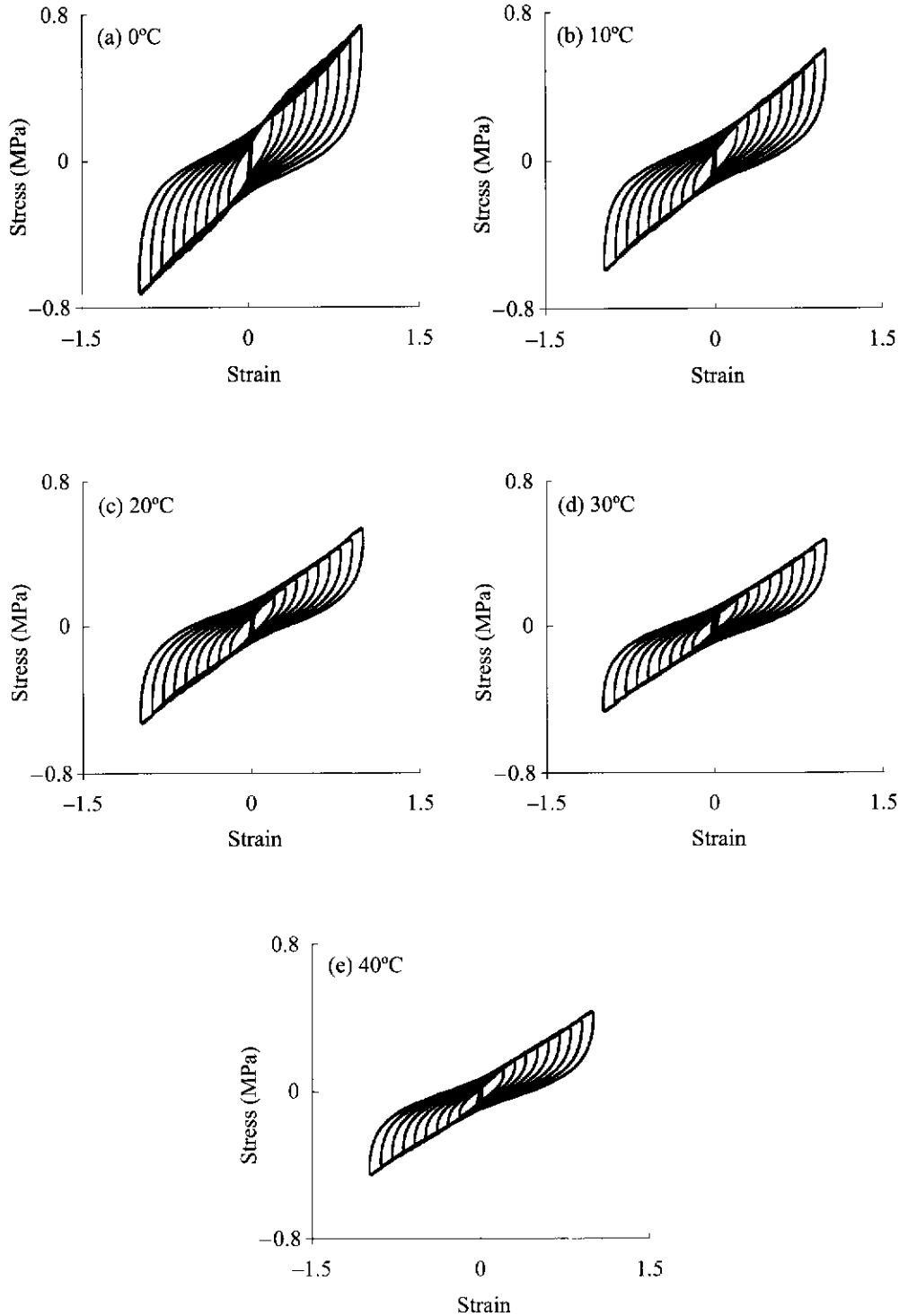

Figure 2. Effect of ambient temperature on hysteresis loops.

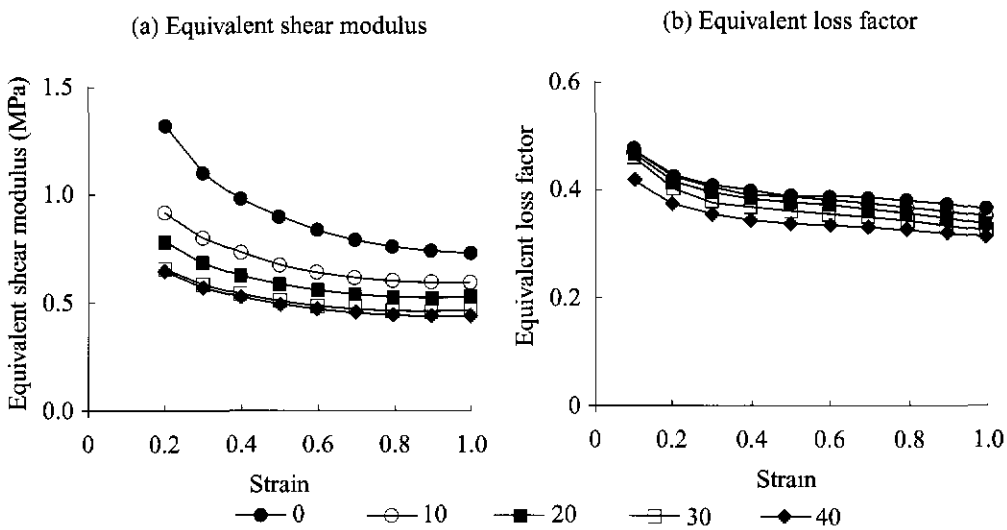

Figure 3. Mechanical properties of UHDNR at various temperatures

temperature than the equivalent shear modulus. A 15% decrease in the equivalent loss factor is observed for all strain amplitudes as the ambient temperature increases from 0°C to 40°C.

The shear strain amplitude dependence on the mechanical properties of UHDNR is shown in *Figure 3*. It is shown in *Figure 3a* that at all ambient temperatures the equivalent shear modulus of UHDNR decreases significantly as the strain amplitude increases from 20% to 40%. The equivalent shear modulus decreases gradually as the strain amplitude increases from 40% to 70%, and does not vary much for strain amplitudes beyond 70%. The equivalent shear modulus at 20% strain amplitude and 0°C is 1.319 MPa, which is about 1.80 times greater than at 100% strain amplitude and 0°C. For other temperatures, the equivalent shear modulus at 20% strain amplitude is 1.40 to 1.54 times greater than at 100% strain amplitude. Compared to the equivalent shear modulus, the equivalent loss factor shows less dependence on strain amplitude. As shown in *Figure 3b*, the equivalent loss factor gradually decreases as the strain amplitude increases. A 20% decrease in the equivalent loss factor is observed at all temperatures as the strain amplitude increases from 20% to 100%.

The equivalent stiffness, G_{eq}, and equivalent loss factor, $\tan(\delta)_{eq}$, obtained from the UHDNR damper tests are tabulated in *Table 1* at various strain amplitudes and ambient temperatures. Rubber-like materials often have a higher stiffness in the first cycle of loading than in subsequent cycles. A decrease in stiffness, known as Mullins's effect[6], occurs over the first few cycles of loading and the hysteresis loops stabilise thereafter. In this study, this stiffness change is ignored, and the mechanical properties shown in *Table 1* are determined from the average of the results from the 4th, 5th,

TABLE 1. MECHANICAL PROPERTIES OF UHDNR DAMPER AT DIFFERENT AMBIENT TEMPERATURES

Temperature	Strain(%)	G_{eq} (MPa)	tan $(\delta)_{eq}$
0°C	0.20	1.319	0.42
	0.30	1.101	0.41
	0.40	0.978	0.40
	0.50	0.897	0.39
	0.60	0.836	0.39
	0.70	0.788	0.38
	0.79	0.760	0.38
	0.90	0.739	0.37
	1.00	0.731	0.36
10°C	0.20	0.918	0.42
	0.30	0.799	0.40
	0.40	0.733	0.39
	0.50	0.676	0.38
	0.60	0.641	0.38
	0.70	0.616	0.37
	0.79	0.602	0.37
	0.90	0.595	0.36
	1.00	0.596	0.35
20°C	0.20	0.782	0.41
	0.30	0.684	0.39
	0.40	0.627	0.38
	0.50	0.588	0.37
	0.60	0.559	0.37
	0.70	0.540	0.36
	0.79	0.528	0.36
	0.89	0.526	0.35
	1.00	0.531	0.33
30°C	0.20	0.657	0.40
	0.30	0.588	0.37
	0.40	0.543	0.37
	0.50	0.512	0.36
	0.60	0.490	0.35
	0.70	0.477	0.35
	0.79	0.466	0.34
	0.90	0.463	0.33
	1.00	0.468	0.32
40°C	0.20	0.646	0.37
	0.30	0.573	0.35
	0.40	0.528	0.34
	0.50	0.495	0.34
	0.60	0.473	0.33
	0.70	0.455	0.33
	0.80	0.445	0.32
	0.90	0.440	0.32
	1.00	0.442	0.31

Tests were performed at 0.5 Hz loading frequency
Values are averages of results for the 4^{th}, 5^{th}, 6^{th}, and 7^{th} cycles among the 10 cycles in each test.

6th, and 7th cycles The equivalent loss factor $\tan(\delta)_{eq}$ for the UHDNR dampers is quite high (about 0 33 to 0 41 at 20°C) compared to HDNR, with an equivalent loss factor in the range of 0 10 to 0 15, used for base isolation bearings[7]

Effect of Loading Frequency

To investigate the effect of loading frequency, the UHDNR dampers were tested at four loading frequencies, 0 5 Hz, 0 75 Hz, 1 Hz, and 1 5 Hz Sinusoidal ten-cycle displacement histories, with each history producing a specified strain amplitude of 25%, 50%, 75%, or 100%. were applied at each loading frequency The hysteresis loops obtained from the experiments are shown in *Figures 4a* to *4d* The corresponding mechanical properties are shown in *Figures 5a* and *5b* As shown in *Figure 4d*, the test data for 100% strain amplitude at 1 5 Hz loading frequency is not included, because the obtained strain (85%) is mush less than the intended strain (100%) due to a limitation in the MTS 810 Material Test System at the ATLSS Center

As shown in *Figures 4a* to *4d*, the variation of loading frequency does not affect the shape of the hysteresis loops However, a slight variation in stiffness was observed as the loading frequency changes The equivalent shear modulus of the UHDNR material increases as the loading frequency increases as shown in *Figure 5a* A 10% increase in stiffness was observed at 25% strain amplitude as the loading frequency increases from 0 5 Hz to 1 5 Hz For 50%, 75%, and 100% strain amplitudes, a 5% to 6% increase in stiffness was observed It is also observed from *Figure 5b* that the equivalent loss factor does not vary much for the range of loading frequencies used in these test

Comparison with Typical Viscoelastic Material

Among many viscoelastic materials, the ISD-110 viscoelastic material produced by the 3M Company has been widely studied as a material for structural dampers for buildings[8-10] The highly damped ISD-110 viscoelastic structural dampers have been shown to significantly decrease lateral drift, base shear, and overturning moment of buildings under dynamic loads such as earthquakes However, the mechanical properties, stiffness and energy dissipation, of the ISD-110 material is excessively sensitive to ambient temperature and loading frequency Research has shown that the design of structural systems with viscoelastic structural dampers may not be effective or satisfactory if the mechanical properties of the viscoelastic material are highly dependent on temperature and frequency[4,10]

The variation of the mechanical properties of the ISD-110 material with ambient temperature and loading frequency is shown in *Figure 6* Unlike the UHDNR material, the ISD-110 material shows high dependence on ambient temperature and loading frequency The variation of the equivalent shear modulus and loss factor with temperature and frequency at 50% strain amplitude is shown in *Figures 6a* and *6b* and at 100% strain amplitude in *Figures 6c* and *6d*

The mechanical properties of ISD-110 material vary significantly with changes in ambient temperature For example, as shown in *Figure 6a*, the equivalent shear modulus at 50% strain amplitude at 15°C is about 11 to 15 times larger than at 40°C The mechanical properties of ISD-110 material are also greatly dependent on the loading frequency as shown When 50% strain amplitude is considered, the stiffness increases due to an increase in loading

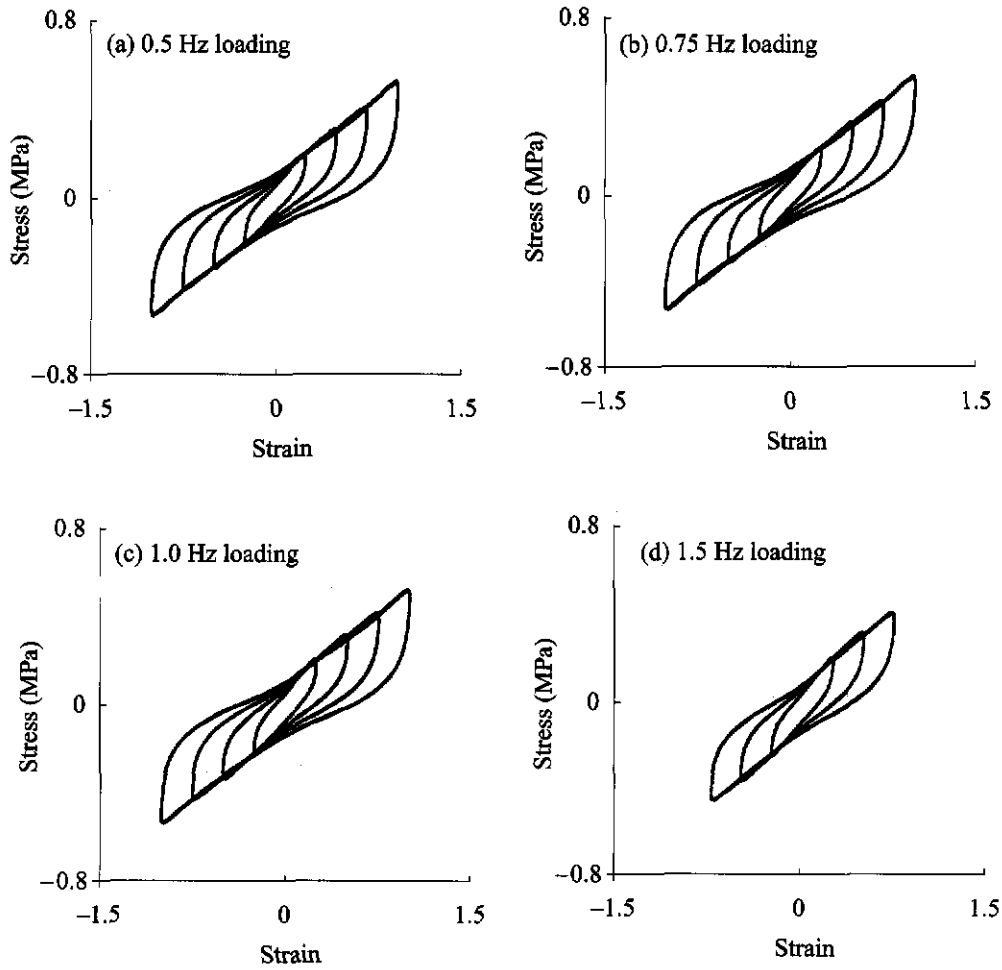

Figure 4. Effect of loading frequency on hysteresis loops at 20°C.

frequency from 0.5 Hz to 2 Hz by a factor of 1.3 to 2.5. Similar to the UHDNR material, the loss factor of the ISD-110 material is less dependent on ambient temperature and loading frequency than the stiffness, as shown in *Figures 6b* and *6d*. Increasing the ambient temperature decreases the loss factor. The loss factor at 50% strain amplitude and 40°C is 59% to 78% of that at 15°C. The variation of the loss factor is larger than that of the UHDNR material.

The excessive sensitivity to ambient temperature and loading frequency of a typical viscoelastic material (ISD-110) makes the design of these viscoelastic structural dampers for buildings more difficult, because the behaviour of the damped system depends

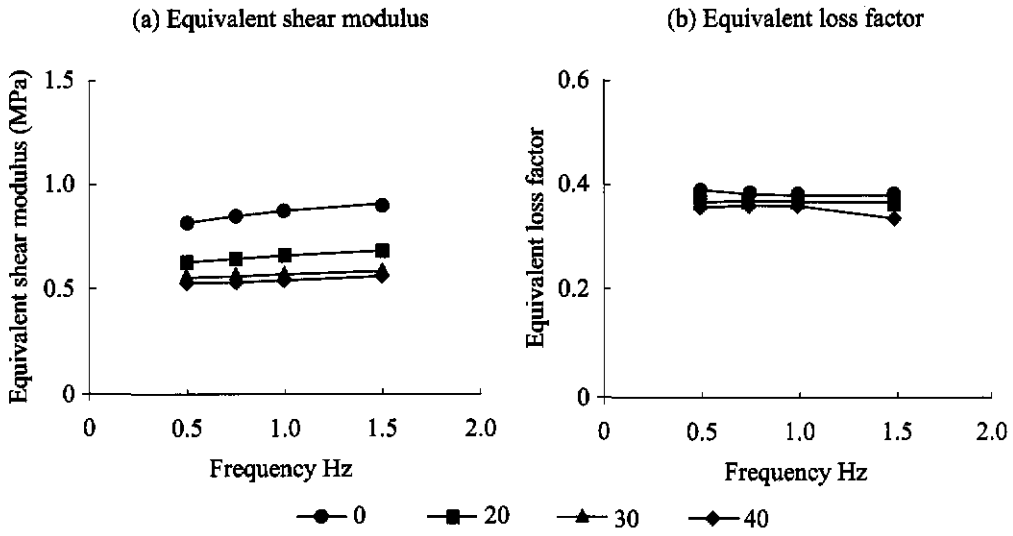

Figure 5. Effect of loading frequency on mechanical properties (20°C).

greatly on ambient temperature and loading frequency.

Rate-dependent Hysteretic Model for UHDNR Dampers

The rate-independent hysteretic model (FPAPM with SAM) proposed by Sause *et al.*[1] were developed to reflect the strain amplitude dependence of UHDNR without consideration of the loading frequency and ambient temperature dependence. Here, this limitation is addressed. First, the loading frequency dependence is included by proposing a loading rate-dependent model, then the ambient temperature dependence is considered.

To represent the frequency-dependent (*i.e.* rate-dependent) hysteretic behaviour of UHDNR under various loading frequencies, a dashpot, graphically shown in *Figure 7*, is added in parallel to the rate-independent model developed previously[1]. As a result, the hysteretic behavior of the rate-dependent model is dependent on both strain amplitude and loading frequency. The stress-strain relationship for the rate-dependent model can be expressed as:

$$\tau(\gamma,t) = \tau_{NL}(\gamma) + \tau_{DP}(t) \quad \ldots 2$$

where $\tau_{NL}(\gamma)$ = the stress-strain function from FPAPM with SAM[1];
$\tau_{DP}(t) = c\dot{\gamma}(t)$; and
c is the coefficient of the dashpot.

In *Equation 2*, the rate-independent part of the model, which is the FPAPM proposed by Sause *et al.*[1], is expressed as:

$$\tau_{NL}(\gamma) = \overline{\tau}(\gamma) - e_0\left[1 - \frac{\overline{W}(\gamma)\,k(\gamma_0 - \gamma)}{e_0}\right]^{-1} \quad \ldots 3$$

where $\overline{\tau}(\gamma)$ = the fourth order polynomial target asymptotes (see Sause *et al.*[1]);

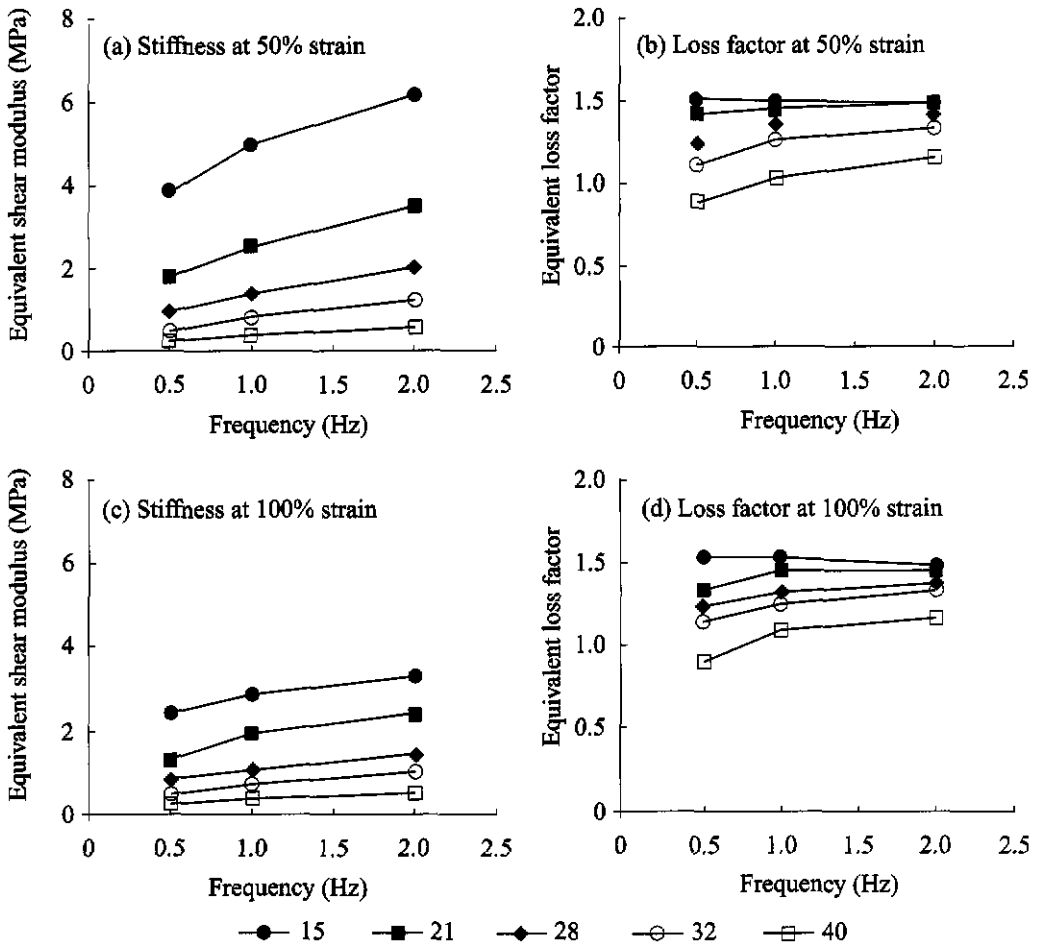

Figure 6. Mechanical properties of ISD-110 viscoelastic material.

$e_0 = \bar{\tau}(\gamma_0) - \tau_0(\gamma_0)$;
for the loading direction,
$\bar{\tau}(\gamma) = \tau_1(\gamma) = A_1\gamma^4 + A_2\gamma^3 + A_3\gamma^2 + A_4\gamma + A_5$; and
$\overline{W}(\gamma) = W_1(\gamma) = A_1[\gamma^3 + \gamma^2\gamma_0 + \gamma\gamma_0^2 + \gamma_0^3] + A_2[\gamma^2 + \gamma\gamma_0 + \gamma_0^2] + A_3[\gamma + \gamma_0] + A_4$;
and for the unloading direction,
$\bar{\tau}(\gamma) = \tau_2(\gamma) = A_1\gamma^4 + A_2\gamma^3 - A_3\gamma^2 + A_4\gamma - A_5$; and
$\overline{W}(\gamma) = W_2(\gamma) = -A_1[\gamma^3 + \gamma^2\gamma_0 + \gamma\gamma_0^2 + \gamma_0^3] + A_2[\gamma^2 + \gamma\gamma_0 + \gamma_0^2] - A_3[\gamma + \gamma_0] + A_4$.

A detailed discussion of *Equation 3* and the SAM model can be found in Sause and co-workers[1]. The rate-dependent model expressed as *Equation 2* has seven parameters, A_1 through A_5 and k (for the rate-independent FPAPM given by *Equation 3*) and c which is the coefficient of the dashpot.

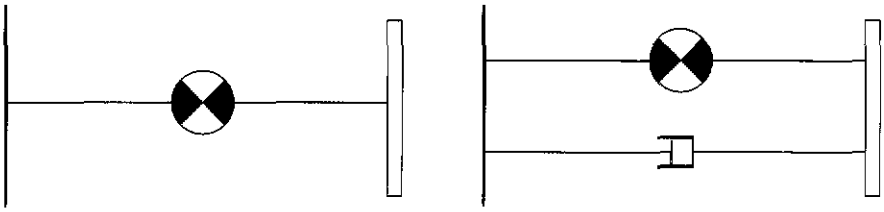

(a) Rate-independent model (b) Rate-dependent model

Figure 7. Rate-independent and rate-dependent model.

The seven parameters for the rate-dependent model in *Equation 2* were determined in the shear stress-strain plane by satisfying the following least-square condition:

$$\text{Minimise } \left\{\sum_{l}\sum_{i}\sum_{j}[\tau_{\exp}(\gamma_{l,i,j}) - \tau_{\mathrm{mod}}(\gamma_{l,i,j})]^2\right\} \quad \ldots 4$$

where l = index for the experimental data set at a specific frequency (*e.g.* $l = 1$, frequency = 0.5 Hz);
i = index for the experimental data set at a specific strain amplitude;
j = index for a stress-strain point within the data set at a specific frequency and strain amplitude;
$\tau_{\exp}(\gamma_{l,i,j})$ = stress data point from the experiments;
$\tau_{\mathrm{mod}}(\gamma_{l,i,j})$ = stress calculated from *Equation 2* using $\gamma_{l,i,j}$ as discussed below; and
$\gamma_{l,i,j}$ = stain data point from the experiments corresponding to $\tau_{\exp}(\gamma_{l,i,j})$.

Since the non-linear regression is performed in the stress-strain plane, the time dependent part of *Equation 2* needs to be modified. When $\gamma(t) = \gamma_i \sin(\omega_l t)$ is applied, the stress in the dashpot can be expressed as:

$$\tau_{DP}(t) = c\omega_l\gamma_i\cos(\omega_l t) \quad \ldots 5$$

where γ_i = the strain amplitude for experimental data set i; and
ω_l = the angular loading frequency for experimental data set l.

Solving $\gamma(t) = \gamma_i \sin(\omega_l t)$ for $(\omega_l t)$ yields:

$$(\omega_l t) = \sin^{-1}\left[\frac{\gamma(t)}{\gamma_i}\right] \quad \ldots 6$$

Substituting *Equation 6* into *Equation 5* gives:

$$\tau_{DP}(t) = c\omega_l\gamma_i\cos\left\{\sin^{-1}\left[\frac{\gamma(t)}{\gamma_i}\right]\right\} \quad \ldots 7$$

The applied strain $\gamma(t) = \gamma_i \sin(\omega_l t)$ can be expressed as $\gamma_{l,i,j}$ at discrete instants in time during a test, where l, i, and j are defined for *Equation 4*. Then *Equation 7* can be written as:

$$\tau_{DP}(t) = (\tau_{DP})_j = c\omega_l\gamma_i\cos\left\{\sin^{-1}\left[\frac{\gamma_{l,i,j}}{\gamma_i}\right]\right\} \quad \ldots 8$$

It is emphasised that *Equation 8* is valid only for the applied strain function, $\gamma(t) = \gamma_i \sin(\omega_l t)$. Substituting *Equation 8* into *Equation 2*, the form of the the rate-dependent hysteretic model needed for the non-linear regression (*Equation 4*) is expressed by:

$$\tau_{\mathrm{mod}}(\gamma,t) = \tau_{NL}(\gamma) + \tau_{DP}(t) = \tau_{NL}(\gamma_{l,i,j}) + c\omega_l\gamma_i\cos\left\{\sin^{-1}\left[\frac{\gamma_{l,i,j}}{\gamma_i}\right]\right\} \quad \ldots 9$$

For an ambient temperature of 20°C, all seven parameters were determined from one non-linear regression. The experimental data shown in *Figure 2c*, from tests at 20°C and various strain amplitudes, and the experimental data shown in *Figures 4a* to *4d*, from tests at 20°C and various frequencies, were included in one non-linear regression to obtain all seven parameters. The Marguadt algorithm[11] was used to determine the parameters. When the regression is performed using the Marquadt algorithm, initial values and ranges for each parameter are necessary. Initial values for some parameters can be estimated from the experimental hysteresis loops. For example, an initial value for A_5 can be estimated from *Figure 2* because A_5 is the intercept with y-axis in the shear stress-strain plane. Also A_4, which is the coefficient of the linear term of the FPAPM, can be estimated from the experimental hysteresis loop. A small value of c is expected because the effect of loading frequency is not significant compared to the effect of strain amplitude on the stress-strain behaviour of UHDNR material. The value for c determined through the non-linear regression is 0.0627 *kN-sec/m* and is tabulated in *Table 3* with the other six parameters.

Comparison of Analytical Results with Experiments

After determining the parameters for the rate-dependent model, typical sinusoidal strain loading histories were used to generate analytical hysteresis loops. The strain amplitudes of the loading were 25%, 50%, 75%, and 100% and the loading frequencies were 0.5 Hz, 0.75 Hz, 1 Hz, and 1.5 Hz. The hysteresis loops from the experiments and the analytical model are compared in *Figures 8a* to *8d*. Good agreement is observed at 0.5 Hz, 0.75 Hz, and 1 Hz loading frequencies for 25%, 50%, 75% and 100% strain amplitudes. The mechanical properties (the equivalent shear modulus and the equivalent loss factor) are compared in *Figures 9a* and *9b*. A small discrepancy in the equivalent shear modulus and the equivalent loss factor at 25% strain amplitude is observed. On the other hand, good agreement is shown for larger strain amplitudes.

Ambient Temperature Effect

As discussed earlier, the behaviour of UHNDR material varies with temperature. Stiffer and fatter hysteretic loops were observed at colder temperatures. For viscoelastic materials, the temperature-frequency equivalence principle[12] is generally used to include ambient temperature effects into analytical models[9,10]. The temperature-frequency equivalence principle relates the stiffness at colder or warmer temperatures to that at a reference temperature by multiplying the model parameters by a shifting factor which is a function of temperature and frequency. However, the application of the temperature-frequency equivalence principle to the rate-dependent model in *Equation 2* is not possible because the rate-independent part of the model, given by *Equation 3*, which is dominant, is not a function of frequency.

In this study, separate non-linear regressions at specific ambient temperatures were performed for the rate-dependent model given by *Equation 2*. The regression performed at 20°C was already discussed. Four more sets of parameters were generated to establish the behaviour of the rate-dependent model at 0°C, 10°C, 30°C, and 40°C. If it were available, experimental data for the strain dependence and frequency dependence of the UHDNR dampers at each temperature could be used for these non-linear regressions. However,

TABLE 2. MECHANICAL PROPERTIES OF UHDNR DAMPER AT DIFFERENT LOADING FREQUENCIES

Frequency	Strain (%)	G_{eq} (MPa)	tan $(\delta)_{eq}$
0.5 Hz	0.25	0.814	0.39
	0.50	0.628	0.37
	0.75	0.551	0.37
	1.00	0.528	0.36
0.75 Hz	0.25	0.847	0.38
	0.50	0.642	0.37
	0.75	0.563	0.37
	1.00	0.532	0.36
1 Hz	0.25	0.873	0.38
	0.50	0.659	0.37
	0.74	0.568	0.37
	0.99	0.535	0.36
1.5 Hz	0.25	0.902	0.38
	0.50	0.683	0.37
	0.73	0.583	0.37
	0.86	0.559	0.34

The ambient temperature was kept at 20°C.

TABLE 3. PARAMETERS DETERMINED FROM NON-LINEAR REGRESSION AT 20°C

Ambient temperature	A_1 (MPa)	A_2 (MPa)	A_3 (MPa)	A_4 (MPa)	A_5 (MPa)	k	c (kN–sec/m)
20°C	–0.177	0.065	0.208	0.316	0.112	21.804	0.063

experiments to investigate the frequency dependence (*i.e.* at various loading frequencies) were performed only at 20°C. From this reason, c is assumed to be temperature independent. This assumption is likely to be acceptable because the frequency dependence of UHDNR is not significant compared to the strain amplitude dependence and the temperature dependence. With a constant value of $c = c_{T=20°C}$ (*i.e.* c determined at 20°C), non-linear regressions were performed to generate parameters for the following equation from the experimental data at 0°C, 10°C, 30°C, and 40°C:

$$\tau_{mod}(\gamma,t) = \tau_{NL}(\gamma) + \tau_{DP}(t) = \tau_{NL}(\gamma_{i,i,j}) + c_{T=20°C}\omega_i\gamma_i\cos\left[\sin^{-1}\left(\frac{\gamma_{i,i,j}}{\gamma_i}\right)\right] \quad \ldots 10$$

The remaining four sets of six parameters at each ambient temperature determined from the non-linear regressions are summarised in *Table 4.*

The hysteresis loops at 0°C, 10°C, 20°C, 30°C, and 40°C from the experiments and the analytical model are shown in *Figures 10a* to *10e.* The hysteresis loops from the

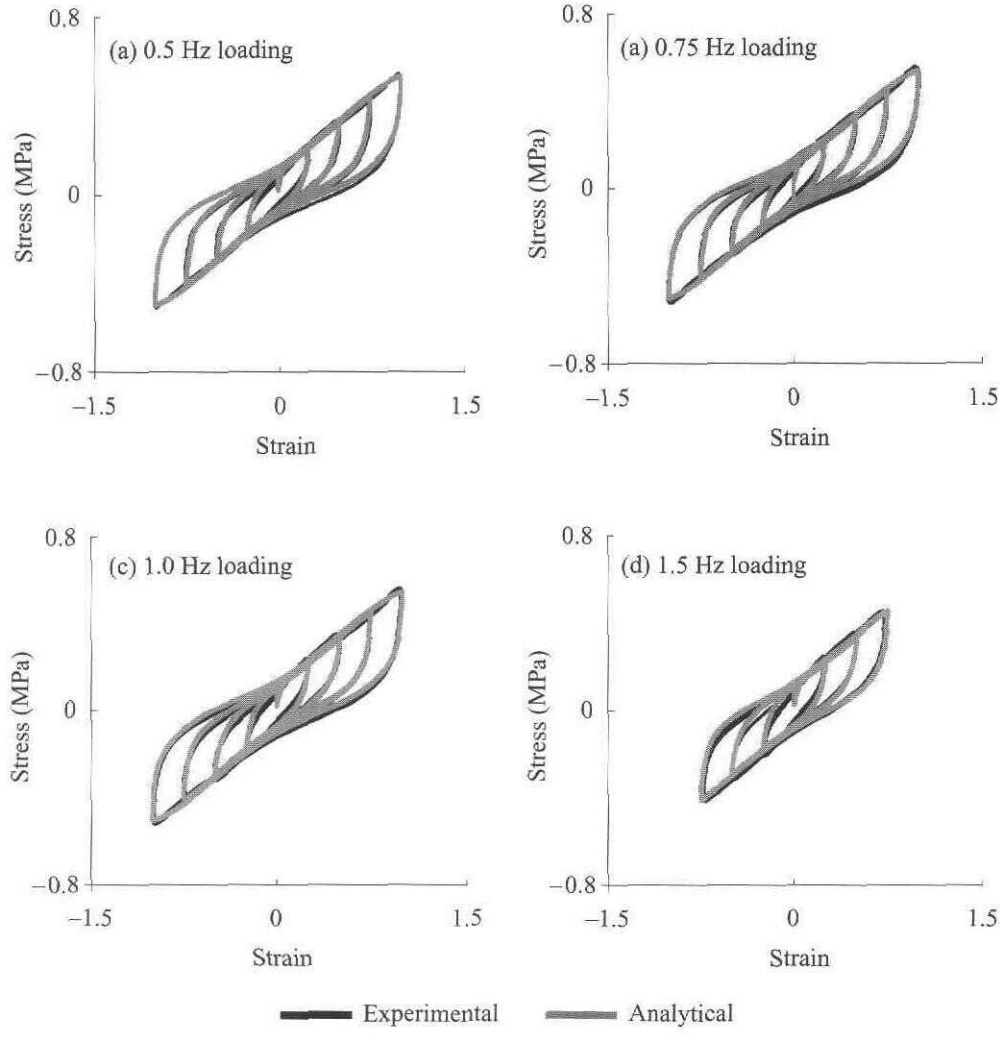

Figure 8. Comparison of hysteresis loops.

experiments and the rate-dependent model at each temperature agree well for all strain amplitudes from 20% to 100%. The mechanical properties at 0°C, 10°C, 20°C, 30°C, and 40°C from the experiments and the analytical model are shown in *Figures 11a* and *11e*. Good agreement of the equivalent shear modulus is observed, but some discrepancy in the equivalent loss factor at small strain amplitudes exists. The discrepancy reduces as strain amplitude increases.

The determined values for the parameters are tabulated in *Table 3* for 20°C and in *Table 4* for other temperatures. The parameter values are plotted in *Figure 12*. As noted above, the

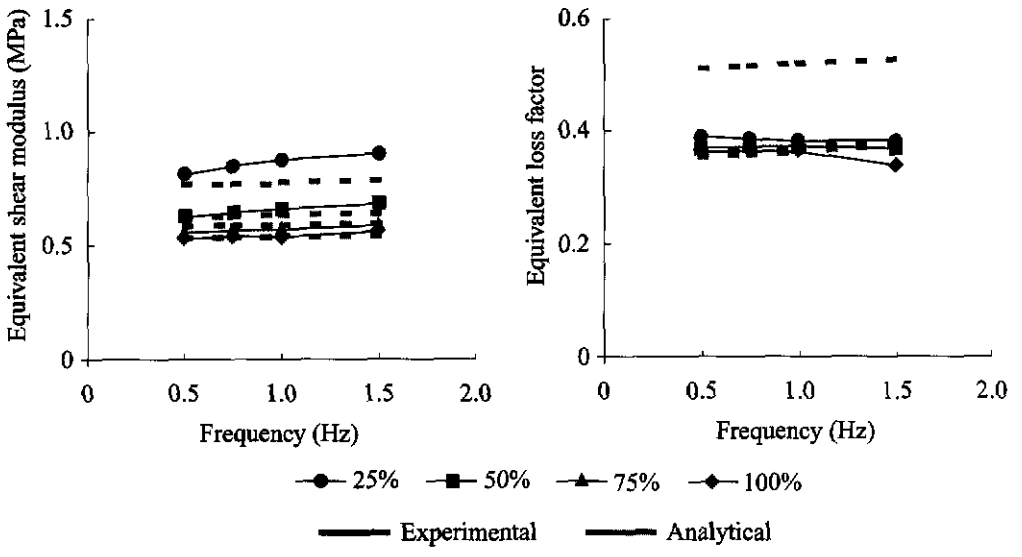

Figure 9. Comparison of mechanical properties.

dashpot coefficient c is constant for all temperatures. Among the other six parameters, A_4 shows the largest change with temperature increase. A_4, the coefficient of linear term in the asymptote function, mainly controls the stiffness. The absolute values of all parameters decrease as ambient temperature increases, and seem to stabilise at 30°C to 40°C. To determine the parameters at intermediate temperatures, such as 5°C, 15°C, 25°C, and 35°C, at which experiments were not performed, regressions of the parameter values were performed as shown in *Figure 13*. The parameters at intermediate temperatures can be determined from the functions tabulated in *Table 5*.

Temperature Increase in UHDNR Due to Loading

Previous studies[9,13] have shown the viscoelastic materials used in structural dampers show a stiffness degradation due to loading history as well as ambient temperature. When structural dampers are under a severe loading condition, the energy dissipated by the material, which is converted to heat, does not dissipate from the material fast enough to prevent a temperature rise that results in stiffness degradation. When the stiffness degradation due to the temperature rise is serious, an analytical model simulating the behaviour of the material should consider this effect.

To evaluate the temperature rise in the UHDNR material and the possibility of an associated decrease in stiffness, sinusoidal loading histories of 100 cycles at 0.5 Hz loading frequency were applied to the UHDNR dampers at strain amplitudes of 25%, 50%, 75%, and 100%. The tests were done at an ambient temperature of 21°C to 23°C. Two thermocouples were installed in the UHDNR material and the temperature increase was monitored during the loading.

TABLE 4. PARAMETERS DETERMINED FROM NON-LINEAR REGRESSION AT 0°C, 10°C, 30°C, AND 40°C

Ambient temperature	A_1 (MPa)	A_2 (MPa)	A_3 (MPa)	A_4 (MPa)	A_5 (MPa)	k	c (kN–sec/m)
0°C	−0.274	0.069	0.304	0.437	0.171	26.599	
10°C	−0.212	0.099	0.232	0.335	0.127	21.348	c_T =20°C
30°C	−0.163	0.082	0.178	0.272	0.087	17.989	=0.0627
40°C	−0.155	0.062	0.170	0.272	0.080	17.083	

TABLE 5. ANALYTICAL EXPRESSION FOR PARAMETERS AS A FUNCTION OF TEMPERATURE

Parameters T = Ambient temperature (°C)	Function
$A_1(T)$	0.00759 ln (T) −0.269 (MPa)
$A_2(T)$	$0.0786\ T^{-0.0603}$ (MPa)
$A_3(T)$	$0.303\ T^{-0.3662}$ (MPa)
$A_4(T)$	$0.429\ T^{-0.3019}$ (MPa)
$A_5(T)$	$0.174\ T^{-0.4691}$ (MPa)
$k\ (T)$	$26.656\ T^{-0.2639}$

The hysteresis loops obtained from these experiments are shown in *Figures 14a* to *14d* for 25%, 50%, 75%, and 100% strain amplitude, respectively. As shown, the stiffness of hysteresis loops gradually decreases as number of loading cycle increases. The effect can be observed more clearly by means of the increase of temperature in UHDNR and variation of the mechanical properties, tabulated in *Table 6*. When the 100-cycle loading history at 25% strain amplitude was applied, the temperature increase due to the loading is less than 2°C, and the decrease in stiffness is about 7% after 100 cycles. The equivalent shear modulus at the end of the 5th cycle was taken as the reference because the results from the first few cycles were not constant due to Mullins's effect[6] as discussed earlier. A 5°C temperature increase and an 8% stiffness decrease were observed for the 100-cycle loading history at 50% strain amplitude. Thus, as a larger strain amplitude is applied, the temperature increase and the stiffness decrease are greater. As shown in *Table 6*, a temperature increase of 7°C and 16°C, and a stiffness decrease of 11% and 16% were observed, respectively, when the 100-cycle loading histories at 75% and 100% strain amplitudes were applied. The 100% strain amplitude test results in the largest temperature increase and stiffness decrease because this test results in the greatest energy dissipation of all of the tests. However, this temperature increase and corresponding stiffness decrease may be ignored in the application of UHDNR structural dampers as follows. When dampers are designed to damp earthquake response in a building, the strain

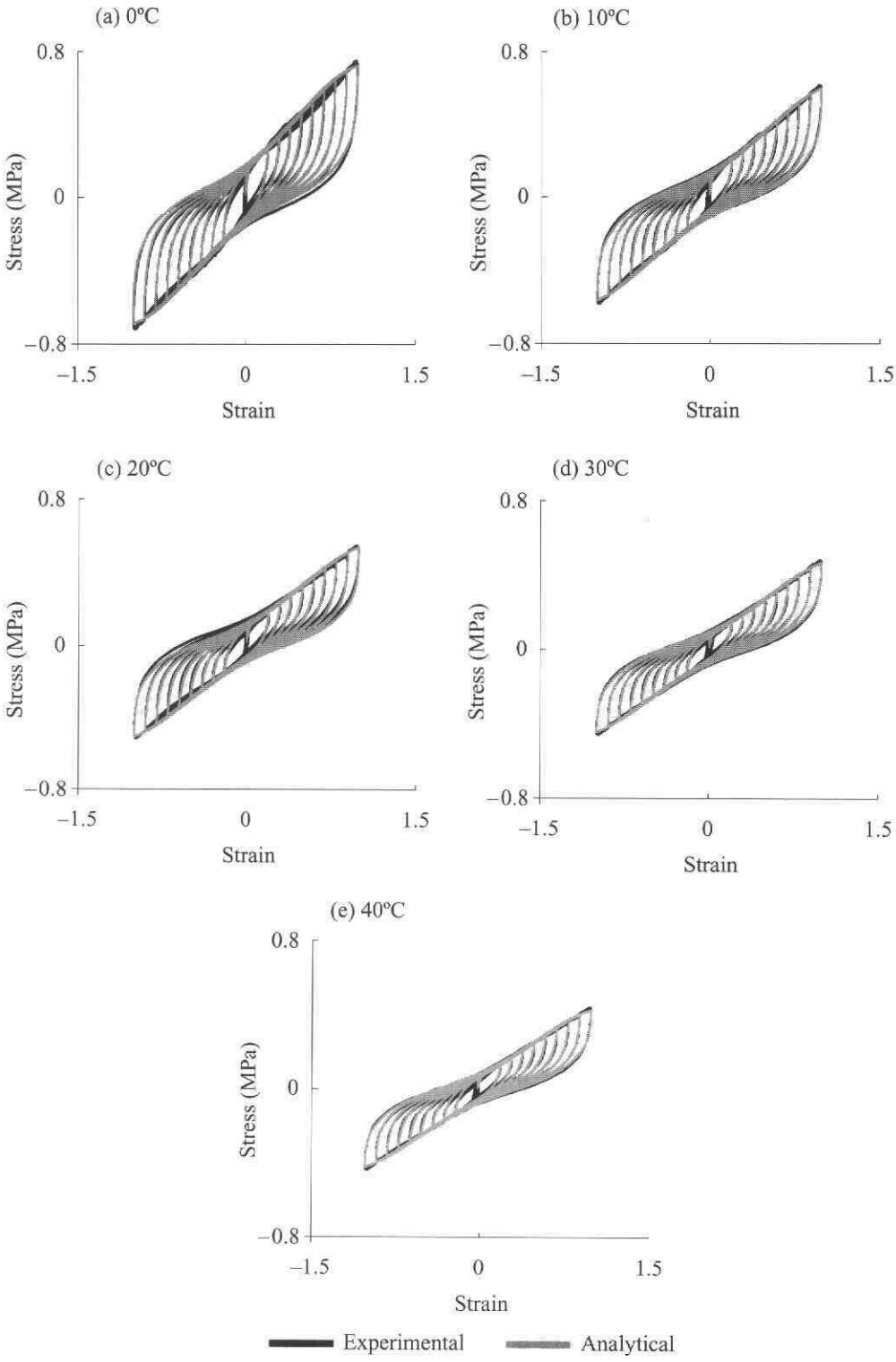

Figure 10. Comparison of hysteresis loops.

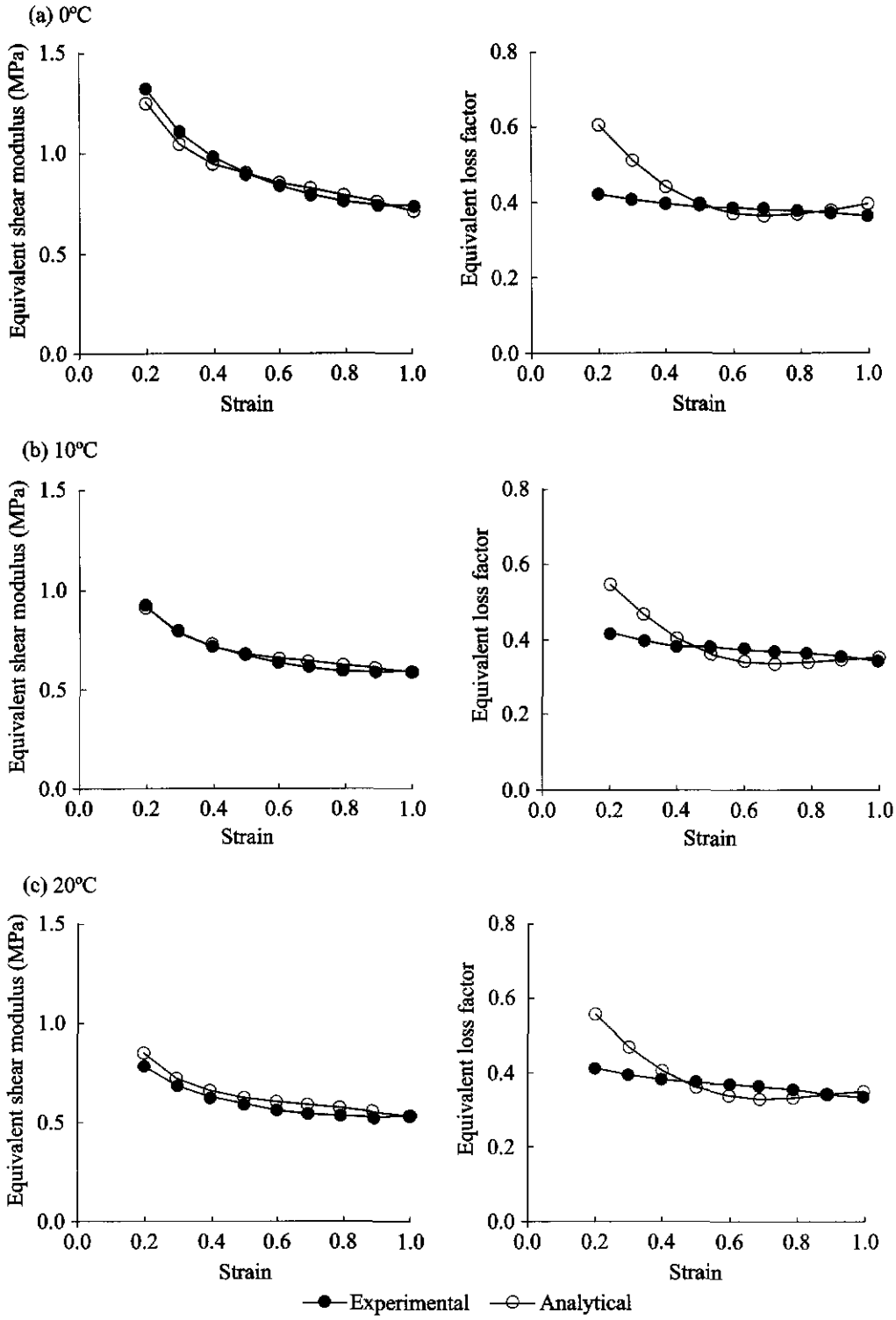

Figure 11. Comparison of mechanical properties at 0°C, 10°C, 20°C, 30°C, and 40°C.

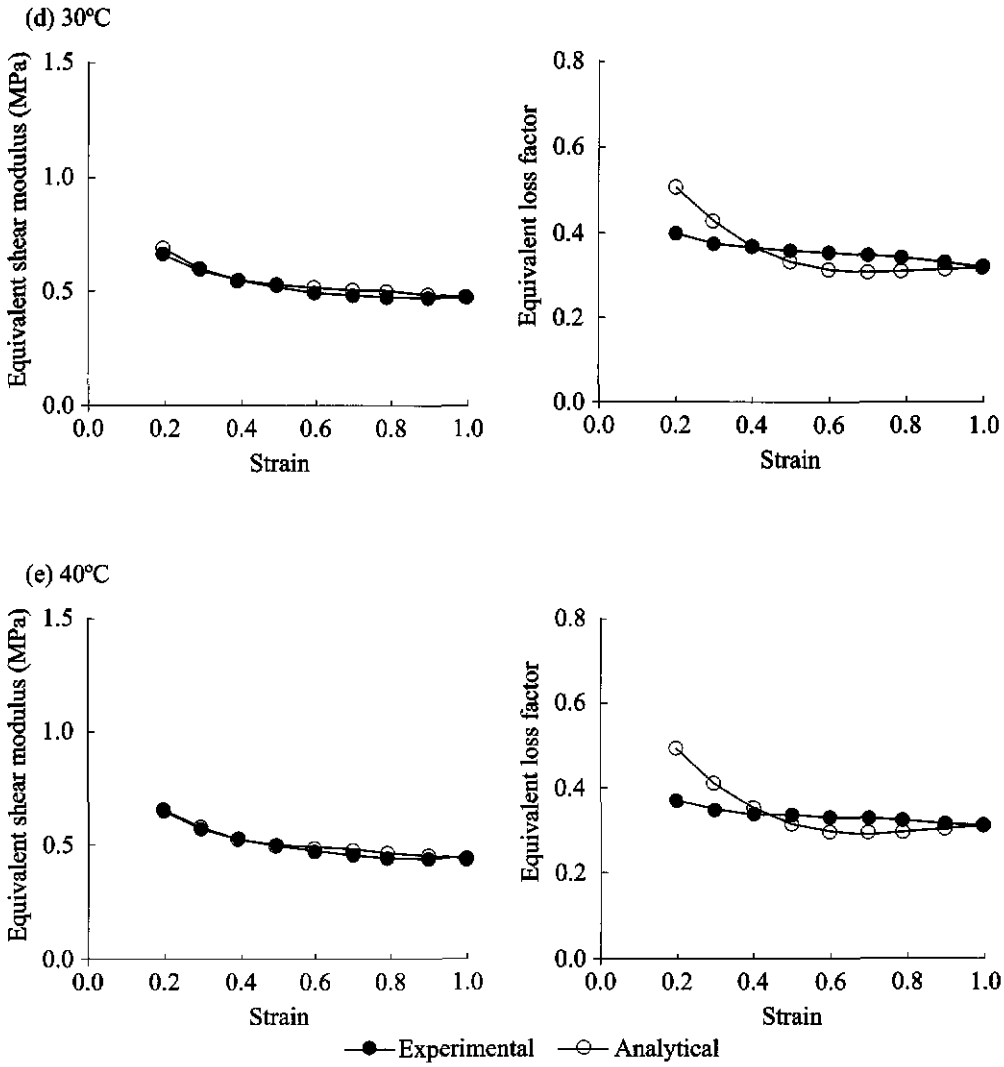

Figure 11. cont.: Comparison of mechanical properties at 0°C, 10°C, 20°C, 30°C, and 40°C.

in the UHDNR is generally limited to 100%. The dampers in a medium rise frame building will oscillate only 30 to 40 cycles under a 30 second earthquake. Conservatively, the mechanical properties at the end of 40 cycles with 100% strain amplitude can be considered as those after an earthquake. As shown in *Table 6*, the decrease in stiffness is 11% and the decrease in loss factor is negligible, which is acceptable for design because the peak responses with large strain amplitudes (*e.g.* 100%) in the dampers will occur only a few times during earthquakes.

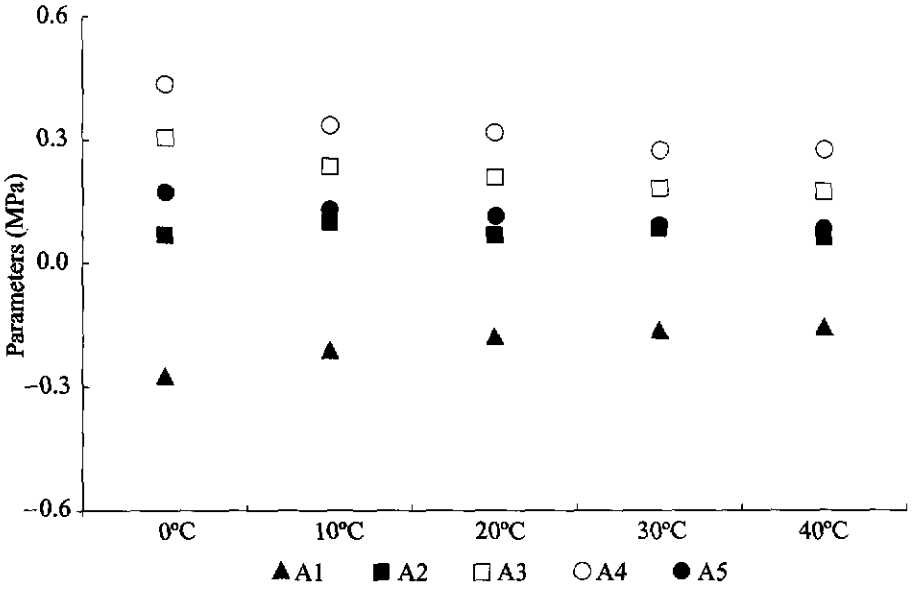

Figure 12. Variation of model parameters with ambient temperature..

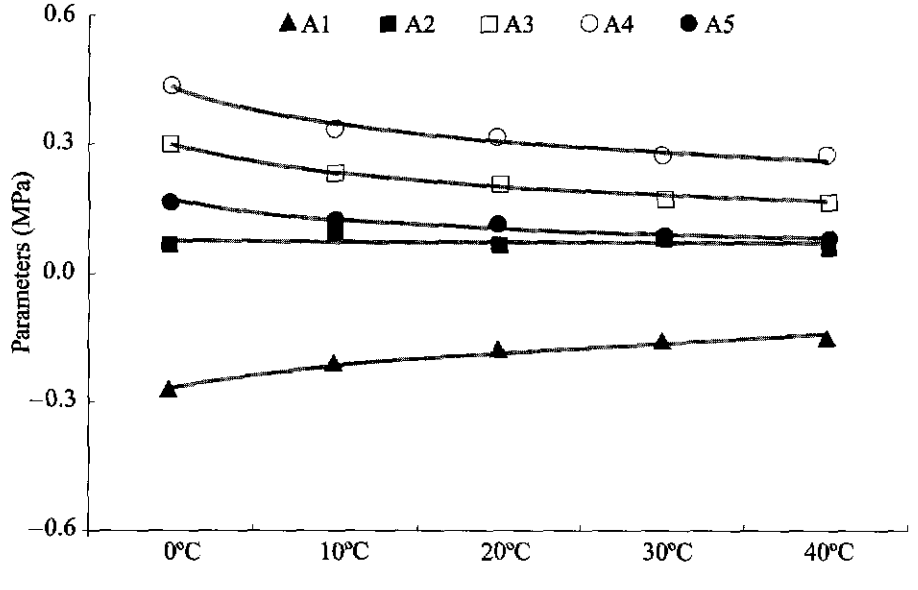

Figure 13. Regression functions fit to parameters.

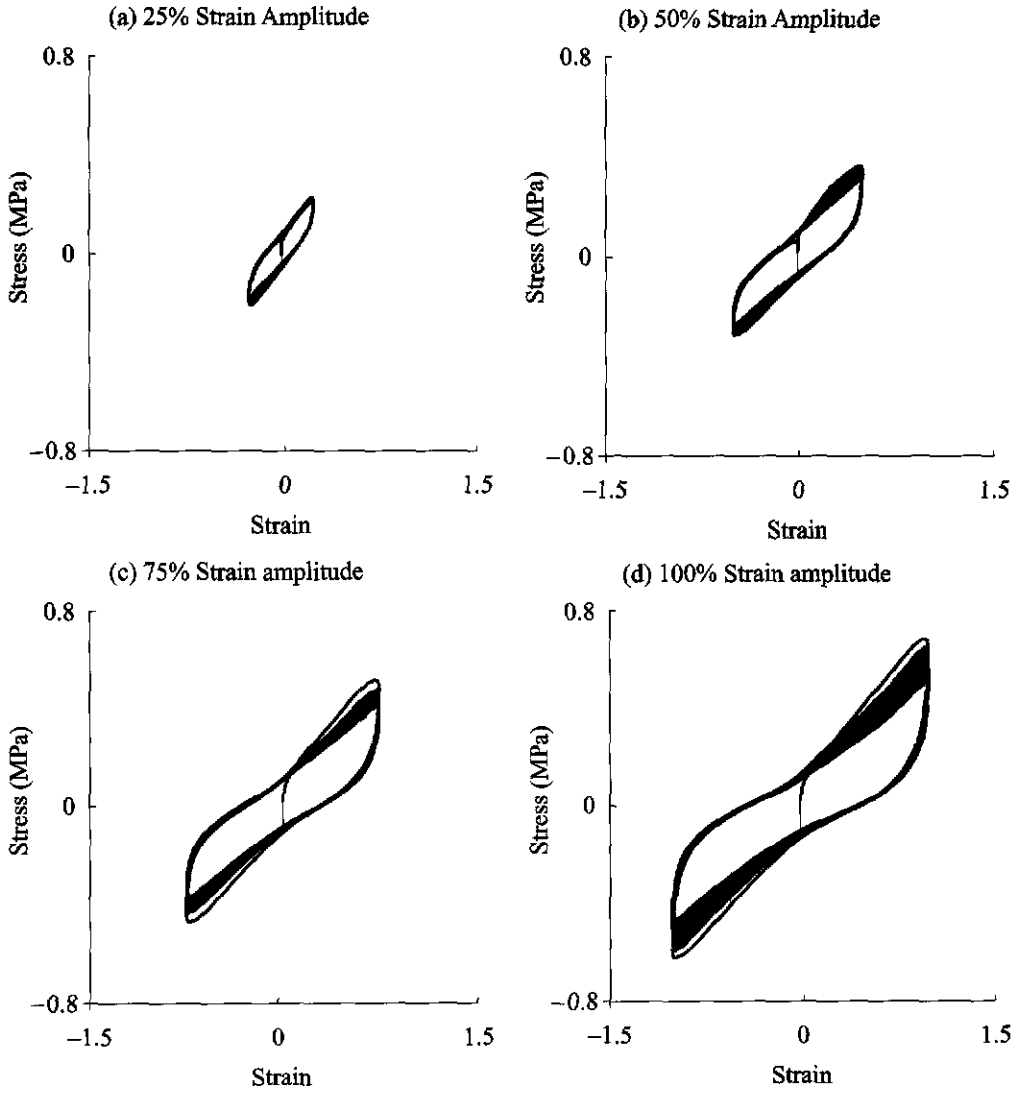

Figure 14. Hysteresis loops of UHDNR damper under 100-cycle loading history at 0.5 Hz loading frequency.

CONCLUSIONS

The mechanical properties of UHDNR material showed dependence on strain amplitude, ambient temperature, and loading frequency. The equivalent shear modulus and the equivalent loss factor of the UHDNR damper were higher at small strain amplitudes. The equivalent shear modulus and loss factor of UHDNR decreased as strain amplitude and ambient temperature

TABLE 6. MECHANICAL PROPERTIES OF UHDNR DAMPER UNDER 100-CYCLE LOADING HISTORY

Strain amplitude	Cycle number	Temp. (°C)	Temp. increase (°C)	G_{eq} (MPa)	$\frac{G_{eq}}{G_{eq}^{5th}}$	$\tan(\delta)_{eq}$	$\frac{\tan(\delta)_{eq}}{\tan(\delta)_{eq}^{5th}}$
25%	0	21.30					
	5	21.42	0.12	0.830	1.00	0.39	1.00
	20	22.03	0.73	0.804	0.97	0.39	0.99
	40	22.39	1.09	0.792	0.95	0.39	0.99
	60	22.63	1.33	0.785	0.95	0.39	0.99
	80	22.88	1.58	0.776	0.93	0.39	0.99
	100	23.00	1.70	0.774	0.93	0.38	0.96
50%	0	22.30					
	5	22.91	0.61	0.628	1.00	0.38	1.00
	20	24.36	2.06	0.605	0.96	0.38	0.99
	40	25.45	3.15	0.594	0.95	0.37	0.98
	60	26.18	3.88	0.586	0.93	0.37	0.98
	80	26.79	4.49	0.584	0.93	0.37	0.97
	100	27.15	4.85	0.580	0.92	0.36	0.95
75%	0	21.80					
	5	23.01	1.21	0.587	1.00	0.36	1.00
	20	25.32	3.52	0.557	0.95	0.36	1.00
	40	26.77	4.97	0.542	0.92	0.36	1.00
	60	27.62	5.82	0.533	0.91	0.36	1.00
	80	28.47	6.67	0.527	0.90	0.35	0.99
	100	29.07	7.27	0.522	0.89	0.35	0.98
100%	0	22.60					
	5	24.90	2.30	0.592	1.00	0.35	1.00
	20	30.00	7.40	0.550	0.93	0.35	0.99
	40	33.63	11.03	0.527	0.89	0.35	0.98
	60	35.94	13.34	0.512	0.86	0.34	0.98
	80	37.63	15.03	0.501	0.85	0.34	0.97
	100	38.97	16.37	0.495	0.84	0.34	0.96

increased. When the loading frequency increased, the UHDNR material stiffness increases, but the loss factor does not change distinctly. The loss factor was less dependant on strain amplitude, ambient temperature, and loading frequency than the equivalent shear modulus. Compared to the viscoelastic material used in structural dampers, the UHDNR showed much less dependence on ambient temperature and loading frequency.

A rate-dependent hysteretic model for the stress-strain behaviour of UHDNR structural dampers was developed by adding a dashpot in

parallel with a rate-independent model[1] The stiffening due to an increase of the loading frequency was modelled For the UHDNR material, the non-linear regression was performed in the stress-strain plane at each ambient temperature. because strain amplitude and ambient temperature dependence dominated the stress-strain behaviour of the material Results from the experiments and the model agreed well at various loading frequencies and ambient temperatures

The temperature increase during loading could be ignored in applications of UHDNR structural dampers to damp the dynamic response of medium-rise frame buildings under earthquakes

ACKNOWLEDGEMENT

The research was conducted at the Center for Advanced Technology for Large Structural Systems (ATLSS) at Lehigh University The authors wish to thank the Malaysian Rubber Board for funding the research The assistance of the ATLSS technical staff, in particular Dr E Kaufmann, E Tomlinson, J Hoffner, J Pinter, and a graduate student. B Metrovich, with the experiments is also acknowledged The opinions expressed in the paper do not necessarily reflect the opinions of those acknowledged here

Date of receipt July 2003
Date of acceptance March 2004

REFERENCES

1 SAUSE R LEE, K-S RICLES J, AB-MALEK, K AND LU, L-W (2001) Non-linear Hysteresis Models for Ultra-high Damping NR Structural Dampers *J Rubb Res*, **4(4)** 222–244

2 AHMADI, H R AND MUHR, A H (1996) Modeling the Dynamic Properties of Filled Rubber *International Rubber Conference Manchester, UK*

3 KIKUCHI, M AND AIKEN, I D (1997) An Analytical Hysteresis Model for Elastomeric Seismic Isolation Bearings *Earthquake Engineering and Structural Dynamics*, **26,** 215–231

4 LEE, K-S (2003) Seismic Behavior of Structures with Dampers Made from Ultra High Damping Natural Rubber Ph D Thesis, Department of Civil and Environmental Engineering, Lehigh University, PA, USA

5 LAZAN, B J (1968) *Damping of Materials and Members in Structural Mechanics*, Oxford Pergamon Press

6 MULLINS L, HARWOOD, J A C AND PAYNE, A R (1967) Stress Softening in Rubbers – A Review *J Instn Rubb Ind*, 1967, **1**, 17–27

7 TANIWANGSA, W, CLARK P W AND KELLY, J M (1996) Natural Rubber Isolation Systems for Earthquake Protection of Low-cost Buildings *Report No UCB/EERC 95-12*, Earthquake Engineering Research Center, University of California, Berkeley, CA USA

8 CHANG, K C, LAI, M L SOONG, T T, HAO, D S AND YEH, Y C (1993) Seismic Behavior and Design Guidelines for Steel Frame Structures with Added Viscoelastic Dampers *Technical Report NCEER- 93-0009*, National Center for Earthquake Engineering Research, State University of New York at Buffalo, USA

9 KASAI, K, MUNSHI, J A, LAI, M L AND MAISON B F (1993) Viscoelastic Damper Hysteretic Model Theory, Experiment, and Application *Seminar on Seismic Isolation Passive Energy Dissipation and Active*

Control Applied Technology Council San Francisco CA pp 521–532

10 FAN, C P (1998) Seismic Analysis, Behavior and Retrofit of Non-ductile Reinforced Concrete Frame Buildings with Viscoelastic Dampers Ph D Thesis Department of Civil and Environmental Engineering, Lehigh University, PA , USA

11 KUESTER, J L AND MIZE, J H (1973) *Optimization Techniques with Fortran*, pp 240–250, New York McGraw-Hill Inc

12 FERRY, J D (1980) *Viscoelastic Properties of Polymers* New York John Wiley and Sons

13 CHANG, K C , TSAI, M H , CHANG, Y H , AND LAI, M L (1998) Temperature Rise Effect of Viscoelastically Damped Structures under Strong Earthquake Ground Motion *Proceedings of the 6th US National Conference on Earthquake Engineering Seattle WA*